Reductive Dehalogenation of Chlorinated Methanes by Iron Metal

Leah J. Matheson and Paul G. Tratnyek*

Department of Environmental Science and Engineering, Oregon Graduate Institute of Science & Technology, P.O. Box 91000, Portland, Oregon, 97291-1000

Reduction of chlorinated solvents by fine-grained iron metal was studied in well-mixed anaerobic batch systems in order to help assess the utility of this reaction in remediation of contaminated groundwater. Iron sequentially dehalogenates carbon tetrachloride via chloroform to methylene chloride. The initial rate of each reaction step was pseudo-first-order in substrate and became substantially slower with each dehalogenation step. Thus, carbon tetrachloride degradation typically occurred in several hours, but no significant reduction of methylene chloride was observed over 1 month. Trichloroethene (TCE) was also dechlorinated by iron, although more slowly than carbon tetrachloride. Increasing the clean surface area of iron greatly increased the rate of carbon tetrachloride dehalogenation, whereas increasing pH decreased the reduction rate slightly. The reduction of chlorinated methanes in batch model systems appears to be coupled with oxidative dissolution (corrosion) of the iron through a largely diffusion-limited surface reaction.

Introduction

In the last few years, new interest in the reactions of reducing metals has been created by contemporary concerns with environmental protection, and an increasing number of research groups are working to assess the utility of these reactions in treatment of contaminated materials. Most of the work reported to date has been focused on reactor design. For example, Senzaki and co-workers (1, 2) reported extensive dehalogenation of 1,1,2,2-tetrachloroethane and trichloroethene (TCE) by iron over a range of conditions in a variety of batch and column reactors. Subsequently, they extended their work, showing that the rate of TCE reduction could be increased by the amalgamation of iron with other metals and that iron surface area seemed to have the greatest influence on the reaction rate (3). A full-scale column reactor has been described by Sweeny (4,5). This device has been tested for treatment of industrial wastewaters using various combinations of Zn, Cu, Al, and Fe mixed with sand. Their systems were reported to dehalogenate trihalomethanes, chloroethenes, chlorobenzene, chlordane, and polychlorinated biphenyls (PCBs) as well as to degrade atrazine, nitrophenols, and N-nitrosodimethylamine. Not all of these reactions were well documented however, and it has been concluded by others that the apparent transformation of PCBs was due to chromatographic effects in the reactor column rather than dechlorination (6).

Another approach to the use of iron metal in environmental remediation originated with a study of groundwater sampling techniques by Gillham and co-workers (7). In that study, it was observed that halogenated hydrocarbon solvents were unstable in the presence of some commonly-used well casing materials. Further investigation of this effect indicated that most of the apparent degradation was due to dehalogenation and that the reaction occurred in the presence of galvanized steel, stainless steel, alu-

minum, and iron. Since iron is relatively inexpensive and nontoxic, it was proposed that it could be useful for the in situ remediation of contaminated groundwaters. Preliminary laboratory tests showed that industrial scrap iron filings produced rapid and extensive reduction of dilute aqueous chlorinated solvents (8, 9). On the basis of these results, a pilot-scale field study was initiated consisting of a permeable barrier, containing iron filings and sand, emplaced perpendicular to the path of an artificial plume of chlorinated hydrocarbons. During the year after installation, the barrier effectively reduced perchloroethylene (PCE) and TCE as evidenced by a roughly stoichiometric increase in dissolved chloride and by identification of trace concentrations of dechlorination products (10).

The success of this field demonstration has attracted considerable attention to the possibility of remediating halocarbon-contaminated groundwaters by dehalogenation with granular iron. Both in situ reactive barriers and above-ground reactors are being developed for this purpose. However, the effective design and operation of these systems will be improved by a more detailed process-level understanding of iron/contaminant interactions in porous media. The purpose of our work in this area is to contribute to such an understanding. In this paper, we describe the mechanism and kinetics of transformations taking place in laboratory model systems containing low concentrations of chlorinated methanes in the presence of granular iron under anaerobic conditions. Further investigations are underway by ourselves and others to address additional transport, geochemical, and microbiological factors that may be important under environmental conditions.

Chemical Background

The redox couple formed by zero oxidation state metallic iron, Fe^0, and dissolved aqueous Fe^{2+}

$$Fe^{2+} + 2e^- \rightleftharpoons Fe^0 \qquad (1)$$
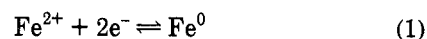
has a standard reduction potential of -0.440 V (11). This makes Fe^0 a reducing agent relative to many redox-labile substances, including hydrogen ions, carbonate, sulfate, nitrate, and oxygen. Alkyl halides, RX, can also be reduced by iron. In the presence of a proton donor like water, they typically undergo reductive dehalogenation:

$$RX + 2e^- + H^+ \rightarrow RH + X^- \qquad (2)$$

The estimated standard reduction potentials of the above half-reaction for various alkyl halides range from $+0.5$ to $+1.5$ V at pH 7 (12). Thus, the net reaction of eqs 1 and 2 is thermodynamically very favorable under most conditions:

$$Fe^0 + RX + H^+ \rightarrow Fe^{2+} + RH + X^- \qquad (3)$$
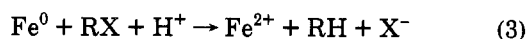
The general reaction represented by eq 3 is a well-known member of a class of reactions known as dissolving metal

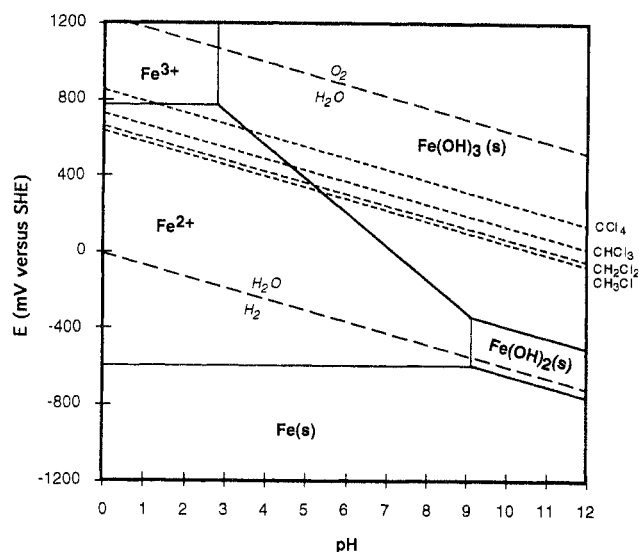**Figure 1.** Pourbaix diagram for the Fe^0-H_2O system under conditions typical of this study: Fe_T = 0.076 mM, {Cl⁻} = 0.001, and 15 °C. Lines for halomethane redox couples are based on potentials in ref 12.

reductions. These reactions have been used in organic synthesis for over 140 years (*13, 14*).

The net reductive dehalogenation by iron (eq 3) is equivalent to iron corrosion with the alkyl halide serving as the oxidizing agent. Since alkyl halides are widely used as solvents and lubricants, their interaction with industrial metals has been of considerable interest. For example, the effect of water on the corrosion of iron and steel by carbon tetrachloride was under investigation as far back as 1925 (*15*). In a series of recent studies using a similar system, corrosion by 11 chlorinated alkanes and alkenes was compared in terms of weight loss of Al, Zn, and Fe (*16, 17*). The reaction rate was found to be greatest for saturated and perhalogenated organic oxidants, with most systems exhibiting accelerated reaction when water was present (*18*).

The characteristic reaction of iron corrosion (eq 1) results in oxidative dissolution of the metal at near neutral pH (*19*). In the absence of strongly oxidizing solutes, there are two reduction half-reactions that can be coupled with eq 1 to produce a spontaneous corrosion reaction in water. Dissolved oxygen, when present, is the preferred oxidant (eq 4) resulting in rapid corrosion according to eq 5:

$$O_2 + 2H_2O + 4e^- \rightleftharpoons 4OH^- \tag{4}$$

$$2Fe^0 + O_2 + 2H_2O \rightleftharpoons 2Fe^{2+} + 4OH^- \tag{5}$$
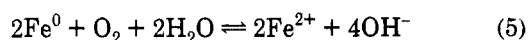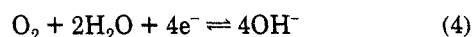
Further oxidation of Fe^{2+} by O_2 leads to the formation of ferric hydroxides (rust). However, water alone can serve as the oxidant (eq 6), and thus, corrosion occurs under anaerobic conditions according to eq 7:

$$2H_2O + 2e^- \rightleftharpoons H_2 + 2OH^- \tag{6}$$

$$Fe^0 + 2H_2O \rightleftharpoons Fe^{2+} + H_2 + 2OH^- \tag{7}$$
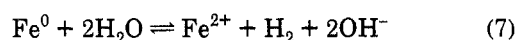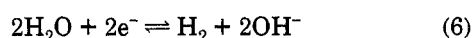
Both reactions (eqs 5 and 7) result in increased pH in weakly buffered systems, although the effect is more pronounced under aerobic conditions because they yield much more rapid corrosion. The pH increase favors the formation of iron hydroxide precipitates (Figure 1), which
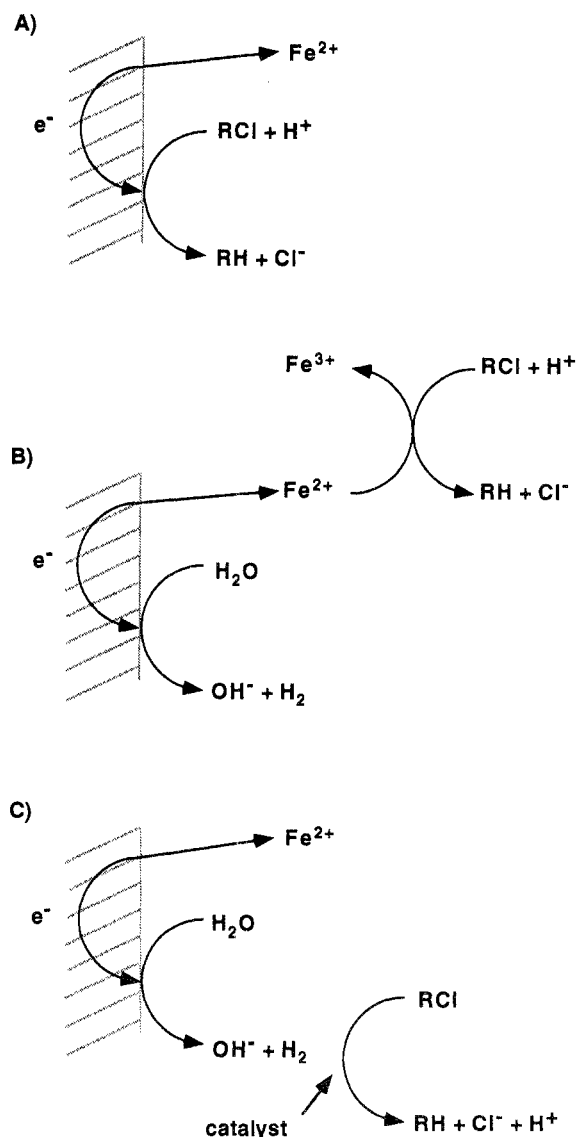

Figure 2. Scheme showing proposed pathways for reductive dehalogenation in anoxic Fe^0-H_2O systems: (A) direct electron transfer from iron metal at the metal surface; (B) reduction by Fe^{2+}, which results from corrosion of the metal; (C) catalyzed hydrogenolysis by the H_2 that is formed by reduction of H_2O during anaerobic corrosion. Stoichiometries are not shown.

may eventually form a surface layer on the metal that inhibits its further dissolution.

The above discussion reveals that the three major reductants in an Fe^0-H_2O system are iron metal and the ferrous iron and hydrogen that result from corrosion. These reductants suggest three general pathways that may be available to contribute to dehalogenation of alkyl halides. The first pathway (Figure 2A) involves the metal directly and implies that reduction occurs by electron transfer from the Fe^0 surface to the adsorbed alkyl halide. Thus, eq 3 alone would describe the reaction pathway.

The second pathway involves the Fe^{2+} that is an immediate product of corrosion in aqueous systems (Figure 2B):

$$2Fe^{2+} + RX + H^+ \rightarrow 2Fe^{3+} + RH + X^- \tag{8}$$

Dissolved Fe^{2+} is a reductant capable of causing dehalogenation of some alkyl halides, although these reactions are generally quite slow (*20, 21*). The importance of this

process will probably be dictated by the ligands present in the system because speciation of ferrous iron significantly affects its strength as a reductant. Inner-sphere complexation of Fe^{2+} to metal oxides can create more reducing species (22), but it is uncertain whether these species can significantly influence rates of dechlorination.

A third model for reductive dehalogenation by iron involves the hydrogen produced as a product of corrosion with water (Figure 2C):

$$H_2 + RX \rightarrow RH + H^+ + X^- \qquad (9)$$
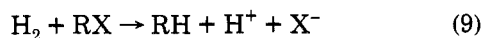
In the absence of an effective catalyst, H_2 is not a facile reductant, and this reaction will not contribute directly to dehalogenation. In fact, excessive H_2 accumulation at the metal surface is known to inhibit the continuation of corrosion and of reduction reactions in organic synthesis. Rapid dehalogenation by H_2 is still possible, however, if an effective catalyst is available (14). The surface of iron, its defects, or other solid phases present in the system could provide this catalysis. Determining the relative importance of these three dehalogenation pathways will be essential to predicting field performance of iron-based remediation technologies.

Experimental Section

Chemicals. Chlorinated solvents were obtained in high purity and used without further purification. These included carbon tetrachloride, HPLC grade (Aldrich); chloroform, LC grade, preserved with 1% (v/v) ethanol (Burdick & Jackson); methylene chloride, 99+%, anhydrous (Aldrich); and trichloroethylene, 99+% (Aldrich). Saturated aqueous stock solutions of these halocarbons were prepared by allowing roughly 1 mL of organic phase to equilibrate with 40 mL of water in glass vials capped with Teflon Mininert valves. Aqueous standard solutions were made by diluting the saturated stock solutions with deionized water (18 MΩ·cm NANOpure).

The iron used in most experiments was an electrolytically-produced 100-mesh powder (Certified Grade, 95%, Fisher) with a nominal S content <0.02%. Our own elemental analysis of the material measured <10 ppm S, 1.3% C, and 0.3% N. Prior to use, fines were removed by sieving with a 325-mesh screen (0.043 mm opening size). After acid pretreatment, the iron had a specific surface area of ≈0.7 m^2/g. Other samples that were tested include "degreased" iron filings (Fisher and EM Science) and iron turnings (>99.9%, Fluka).

Buffers were reagent-grade and used as received (Sigma). These included 2-(N-cyclohexylamino)ethanesulfonic acid (CHES); N-(2-hydroxyethyl)piperazine-N'-2-ethanesulfonic acid (HEPES); 2-(N-morpholino)ethanesulfonic acid (MES); 3-(N-morpholino)propanesulfonic acid (MOPS); and tris(hydroxymethyl)aminomethane (Tris). Anaerobic solutions of all media were prepared by purging for roughly 1 h with zero-grade N_2 that was deoxygenated by passing through a heated column of reduced copper.

Model Reaction Systems. Dechlorination experiments were performed in closed batch systems prepared in 60-mL serum bottles. In most cases, each bottle received 1 g of iron, weighed dry to the nearest milligram. Oxides and other surface coatings were removed by exposing the iron sample to 10 mL of 3% HCl for 1 h and then rinsing three times with deoxygenated deionized water while purging the open bottle with N_2. Serum bottles containing

acid-washed iron were then filled completely with deoxygenated deionized water or an appropriate buffer solution and crimp-sealed with Hycar septa (Pierce). No evidence for ferric oxide precipitation was found, even by optical microscopy. Loss of substrate to Hycar septa was less than 10% for carbon tetrachloride after 2 days and 20% for chloroform, 10% for dichloromethane, and 25% for trichloroethylene after 17 days. Each bottle was allowed to equilibrate for 8–12 h on a rotary shaker (15 rpm) in a dark, 15 °C room before addition of the substrate. A temperature of 15 °C was chosen for the dechlorination experiments to reflect common groundwater conditions.

To initiate a dechlorination experiment, 2 mL of a saturated aqueous halocarbon stock solution was added by injection through the septum. A second needle was used to allow an equal volume of water to be displaced, so each dechlorination experiment began at 1 atm pressure with no headspace. Typical concentrations were 100–200 μM for carbon tetrachloride, 100–200 μM for chloroform, and 100–800 μM for dichloromethane. Reaction conditions were usually the same as those for the equilibration step described above. Loss of parent compound and production of dechlorinated product were determined by periodically removing 2.0-μL samples for immediate analysis using the methods described below.

Analyses. Two chromatographic methods were used to determine the aqueous concentration of chlorinated solvents. Initial work employed purging with whole-column cryotrapping (23) with FID detection. However, most work was done by a modification of the method for direct aqueous injection on capillary columns developed by Grob (24). Samples (2 μL), taken directly from the reaction bottles, were injected via an on-column inlet at 92 °C, to a 2.5 m × 0.53 mm i.d. precolumn attached to a 30 m × 0.53 mm i.d. DB 624 analytical column (J&W) in an oven heated to 104 °C. Satisfactory results were obtained with detection by FID. Peaks were identified by comparison with the retention times of standard compounds. A dedicated chromatograph for headspace reducing gases was used to verify that H_2 was produced by anaerobic corrosion (Trace Analytical).

A variety of techniques were used to characterize the iron samples used in this study. Total carbon, nitrogen and sulfur contents of the metal were determined using a dedicated elemental analyzer by complete combustion with thermal conductivity detection (Carlo Erba NA-1500). The detection limit for sulfur (as SO_2) with this instrument was 10 μg/mg dry weight of sample. Iron surface area was determined by gas adsorption (Micromeritics, Gemini 2360) on samples that had been rinsed with methanol and dried under N_2 gas. Scanning electron microscopy was performed on a Zeiss 960 digital SEM with elemental analysis by energy-dispersive X-ray spectroscopy. The production of dissolved iron was quantified with the ferrozine method (25).

Determinations of pH before and after each experiment were made in open bottles with a gel-filled combination electrode. Measurements during an experiment were made through the septum with an 18-gauge, beveled tip combination electrode (Microelectrodes, Inc.). Two-point calibrations were performed daily at pH 4.00 and 7.00 using commercial buffers. Eighteen-gauge needle-form combination electrodes (Microelectrodes, Inc.) were also used to measure redox potential. The platinum element was conditioned in dilute nitric acid, and the electrode

performance was verified in a solution of iron ammonium sulfate (26). Electrode potential was measured in the sealed serum bottles and is reported in volts versus the standard hydrogen electrode (SHE).

Results and Discussion

Corrosion in Fe⁰–H₂O Model Systems. About 15% of the iron used to start each experiment was lost by corrosion during the acid pretreatment step. Corrosion continued after rinsing the iron and reconstituting the system at circum-neutral pH. However, iron dissolution was much slower under these conditions, as evidenced by the lack of measurable decrease in iron by weight and the production of <400 $\mu g/L$ Fe^{2+}. The concentration of H_2 increased to >400 mg/L within 1 h, confirming that anaerobic corrosion was taking place by the reduction of water (eq 7). The pH did not increase significantly, suggesting that the hydroxide produced by water reduction was balanced by other processes, perhaps formation of iron hydroxides.

Values of the Pt electrode potential measured in the solution decreased rapidly after the system was sealed and mixed. After the initial rapid decline, the potential continued to decrease but much more slowly. This decrease continued throughout the equilibration period to a value of approximately -300 mV (vs SHE). The trend reflects a gradual dissolution of Fe^0 to give Fe^{2+} (Figure 1). Ferrous iron has a large exchange current with Pt and is undoubtedly the dominant electrode-active species in this system. When carbon tetrachloride was added through the septum, the electrode potential increased sharply, about 100 mV, but then declined rapidly to its prior value.

The 8–12 h equilibration period between setup and initiation of dechlorination experiments was intended to ensure that our model systems reflect the behavior of iron in long-term field applications and not initial adjustments in conditions like the rapid decrease in electrode potential described above. However, dechlorination rates were generally the same whether the substrate addition was made immediately after setup or after the equilibration period of approximately 8 h.

Halocarbon Degradation Pathways. There are several general reaction types available for cleaving the carbon–halogen bonds that characterize many environmental contaminants. These include nucleophilic substitution by water or hydroxide (hydrolysis) or by sulfide or thiols; β-elimination of HX (dehydrohalogenation); *gem*-elimination yielding products via a carbene intermediate; reductive elimination of adjacent halogens leaving an unsaturated product (vicinal dehalogenation); reduction of a single C–X bond to a C–H bond (reductive dehalogenation, eq 2); and oxidation to carbonyl products (12, 27, 28). The relative rates of these processes will vary with substrate and chemical and microbiological conditions. Halogenated methanes are not subject to dehydrohalogenation or vicinal dehalogenation, and hydrolysis of these compounds is very slow under most conditions (29). Carbon tetrachloride was chosen as the primary substrate for this study, in part, to be able to focus on reductive dehalogenation in the presence of iron. Many previous studies have used carbon tetrachloride as a model compound with which to study the reductive dehalogenation as an environmental pathway (30, 31).
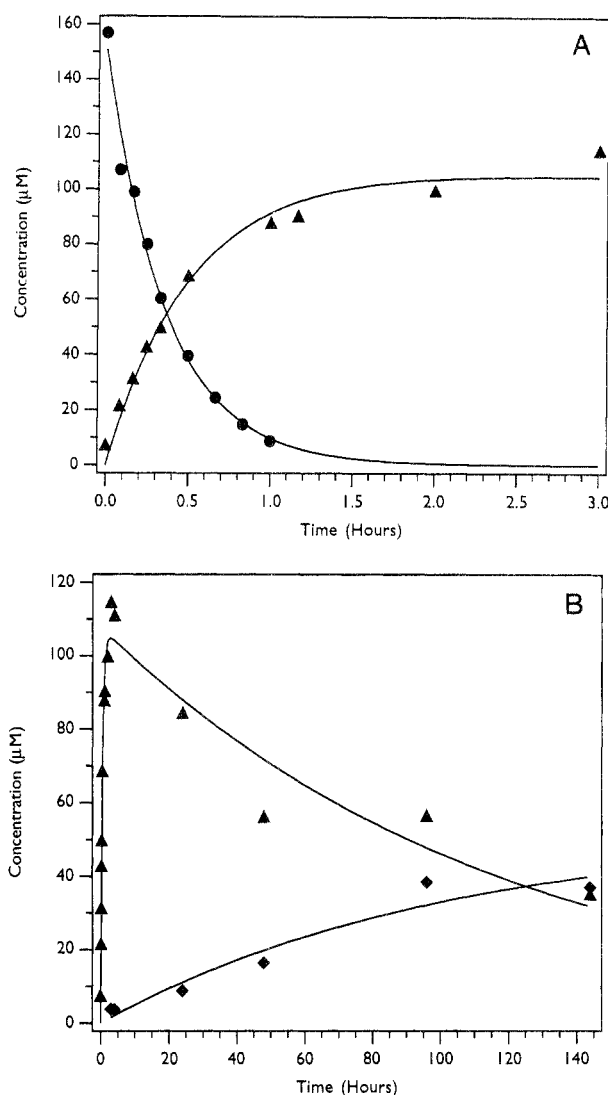
Figure 3. Disappearance of (A) carbon tetrachloride and (B) chloroform, with the appearance of corresponding sequential dehalogenation products. System: 1 g of iron, unbuffered pH 8.0, and 15 °C. (●) carbon tetrachloride; (▲) chloroform; (♦) methylene chloride.

Carbon tetrachloride was found to be degraded by reductive dehalogenation to chloroform in all systems containing iron metal. Conversion to chloroform typically accounted for about 70% of the carbon tetrachloride lost (Figure 3A). After the carbon tetrachloride concentration had decreased to the detection limit, methylene chloride was observed from further reductive dehalogenation of chloroform (Figure 3B). The appearance of methylene chloride typically accounted for about 50% of the chloroform lost. Methylene chloride disappearance was only apparent after several months, and it was not possible to unequivocally demonstrate that this was a result of dechlorination. No formation of chloromethane, methane, or coupling products like hexachloroethane were detected. Analyses for formate or chloride were not performed. The results indicate that the dominant degradative pathway for chlorinated methanes in anaerobic Fe^0–H_2O systems is sequential reductive dehalogenation and that the rates become much less favorable with each successive dechlorination step. A few similar experiments were performed with TCE as substrate. TCE was degraded, but the products of this reaction were not investigated.

Kinetics of Transformation. In well-mixed systems, plots of the natural logarithm of substrate concentration

Table 1. Kinetics of Carbon Tetrachloride Disappearance[a]

RX	$[RX]_{max}$ (μM)	k_1 (min^{-1})	k_2 (min^{-1})
CCl$_4$ (eq 10)	151 ± 5	0.045 ± 0.003	
CHCl$_3$ (eq 11)	107 ± 1	0.032 ± 0.005	(1.41 ± 0.03) × 10^{-4}
CH$_2$Cl$_2$ (eq 12)	53 ± 18		(1.6 ± 0.9) × 10^{-4}

[a] Experiment performed at 15 °C and 15 rpm using 1.00 g of iron. Uncertainties are 1 SD in the fitted parameter from nonlinear regression.

Table 2. Effects of Treatments on Rate of Reductive Dehalogenation for Carbon Tetrachloride[a]

Fe (g)	FeCl$_2$ (mg/L)	H$_2$ (psi)	EDTA (mM)	k_{obs} (min^{-1})[b]
1.00			0	0.062
1.00		10	0	0.083
1.00	5		0	0.037
1.00	50		0	0.049
1.00	100		0	0.024
1.00	100		0.5	0.030
1.00			0.5	0.061
0		10	0	ND[c]
0	100		0	ND[c]
0	100		0.5	ND[c]

[a] Conditions: unbuffered pH ≈ 7, 15 °C, 15 rpm, 100-mesh Fisher electrolytic iron. [b] Uncertainties from the regression lines are <0.008 min^{-1} (±1 SD) for all cases. [c] ND, no detectable loss.

versus time for carbon tetrachloride and chloroform gave straight lines from their initial concentrations to their respective minimum detection limits (1–3 half-lives, typical $r^2 > 0.95$ for $n = 5$–10). From this, it was concluded that the kinetics of these reactions are pseudo-first-order in substrate and that the various possible changes in the system—due to the simultaneous corrosion of iron—did not significantly affect dechlorination rates over the duration of our experiments. The slope of lines regressed to natural logarithm of concentration versus time data were used to obtain first-order rate constants, k_{obs}, in most of the experiments reported below. However, to illustrate the entire time course of one experiment, the data in Figure 3 have been fit by nonlinear regression to the integrated rate laws for sequential first-order reactions (32):

$$[CT]_t = [CT]_{max} e^{-k_1 t} \quad (10)$$

$$[CF]_t = \frac{[CF]_{max} k_1}{k_2 - k_1}(e^{-k_1 t} - e^{-k_2 t}) \quad (11)$$

$$[MC]_t = [MC]_{max}(1 - e^{-k_2 t}) \quad (12)$$

where k_1 is the first-order rate constant for dechlorination of carbon tetrachloride (CT) to chloroform (CF) and k_2 is the rate constant for conversion of chloroform to methylene chloride (MC). The results of these calculations are presented in Table 1. The disappearance rate constant for carbon tetrachloride corresponds to a $t_{1/2} = 15$ min, which is typical of unbuffered experiments run at 15 rpm using 1.00 g of acid-washed Fisher electrolytic iron. Under these conditions, chloroform disappearance occurs with $t_{1/2} \approx 3$ days, and methylene chloride is not measurably degraded. Note that the concentration of chloroform in Figure 3 reflects both dehalogenation from carbon tetrachloride to chloroform and subsequent dechlorination of chloroform to dichloromethane. The differences between corresponding parameters in Table 1 are consistent with incomplete mass balances at each dechlorination step, as described above. The rate of trichloroethylene disappearance in our model system was first-order in substrate concentration with a $t_{1/2} = 30$–40 days (data not shown).

Pathway of Dechlorination by Iron. As illustrated in Figure 2, the presence of iron metal, Fe^{2+}, and H$_2$ in anaerobic Fe^0–H$_2$O systems provides three possible reducing agents capable of effecting dehalogenation. A variety of control experiments and treatment studies were performed to help identify which of these reductants is the most important contributor to the transformation of carbon tetrachloride, and the results are summarized in Table 2. Uncatalyzed reduction by dissolved H$_2$ or Fe^{2+} can be excluded on the basis of control experiments: neither H$_2$-saturated water nor 5–100 mg/L FeCl$_2$ produced measurable dehalogenation over 15 days in the absence of the metal. It is difficult to exclude the possibility that

adsorbed Fe^{2+} or nascent hydrogen that results from reduction of water at the iron surface may be participating in the dehalogenation reaction. However, amendment of Fe^0–H$_2$O systems with additional Fe^{2+} or H$_2$ did not affect the rate of carbon tetrachloride dehalogenation in a significant or systematic manner. In addition, 0.5 mM EDTA, which should form a redox-inactive complex with Fe^{2+} produced by corrosion (33), had no effect on the carbon tetrachloride dehalogenation rate. Taken together, the data in Table 2 suggest that reductive dehalogenation directly coupled with oxidative dissolution of the metal (Figure 2A) is the dominant process under conditions employed in this study.

Effect of pH. Understanding dehalogenation by iron as reduction of the halocarbon coupled with oxidative dissolution of the metal suggests several ways in which pH may influence the reaction rate. The requirement for H$^+$ participation in the overall reaction (eq 3) suggests the possibility that protons may appear in one or more elementary steps that influence the reaction rate directly. In addition, strong indirect effects are possible due to increased aqueous corrosion at low pH or iron hydroxide precipitation at high pH. Our early experiments showed that unbuffered systems consistently gave pH values of 7.5–8.0 and that changes during the course of carbon tetrachloride dehalogenation experiments were small: pH typically decreased, but by less than 1 unit. Since this modest variability in pH did not appear to be affecting dehalogenation rates, most experiments were carried out without added buffer.

To determine the carbon tetrachloride dehalogenation rate over a wide range of pH, a series of buffered systems was needed. Good's buffers were used because they interact weakly with most metals in solution (34), and preliminary tests gave no visual evidence for precipitation with iron over the duration of a typical experiment. Five of these buffers with overlapping pH ranges were used to obtain data from pH 5.5 to 10.0 (Table 3). The values of k_{obs} decreased with increased pH, and the trend showed no inconsistencies attributable to individual buffers (Figure 4). Unbuffered systems gave dehalogenation rates consistent with buffered systems at similar pH values. The effect of pH on k_{obs} is apparently linear; giving a least-squares regression line of

$$k_{obs} = -0.018 \, (\pm 0.001) \, \text{pH} + 0.20 \, (\pm 0.01) \quad (13)$$

with $r^2 = 0.92$ for $n = 16$. The slope of this line has been useful for estimating the potential significance of pH

Table 3. Kinetics of Carbon Tetrachloride Disappearance in Buffered Systems[a]

Fe (g)	pH	buffer type	k_{obs} (min^{-1})[c]
1.00	6.5[b]	MOPS	0.083
1.00	7.4	MOPS	0.067
1.00	8.2	MOPS	0.041
0	7.4	MOPS	0
1.00	6.4[b]	HEPES	0.080
1.00	7.5	HEPES	0.060
1.00	8.2	HEPES	0.047
0	7.5	HEPES	0
1.00	5.5[b]	MES	0.100
1.00	6.0[b]	MES	0.088
1.00	6.6[b]	MES	0.083
0	6.0	MES	0
1.00	8.6	CHES	0.037
1.00	9.0	CHES	0.036
1.00	9.5	CHES	0.037
1.00	10.0	CHES	0.026
0	9.0	CHES	0
1.00	7.2	Tris	0.077
1.00	8.0	Tris	0.053
1.00	9.0	Tris	0.018
0	8.9	Tris	0

[a] Conditions: 15 °C, 15 rpm, 100-mesh Fisher electrolytic iron, 50 mM buffer. [b] pH decreased due to rapid corrosion despite buffer. [c] Uncertainties are <0.01 based on slope of the regression line.

Figure 5. Effect of surface area on pseudo-first-order rate constants for carbon tetrachloride dehalogenation. Iron weights varied, as shown in Table 3. The systems were unbuffered mixed at 15 rpm and incubated at 15 °C. Regression line corresponds to eq 14. Solid circles are the fitted data; open circles are data collected in a subsequent experiment to validate the results by varying reaction volume.
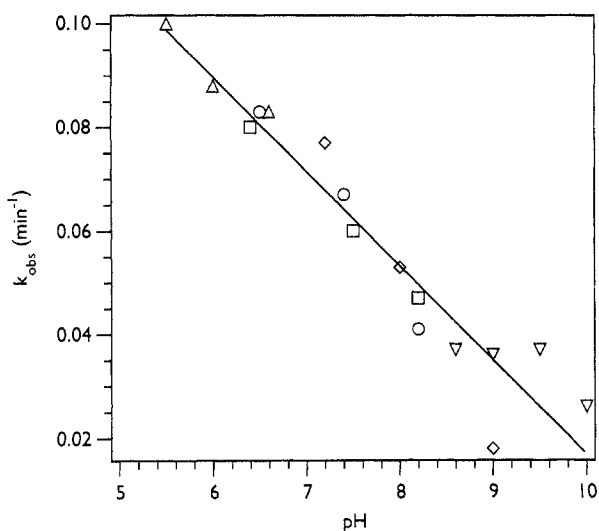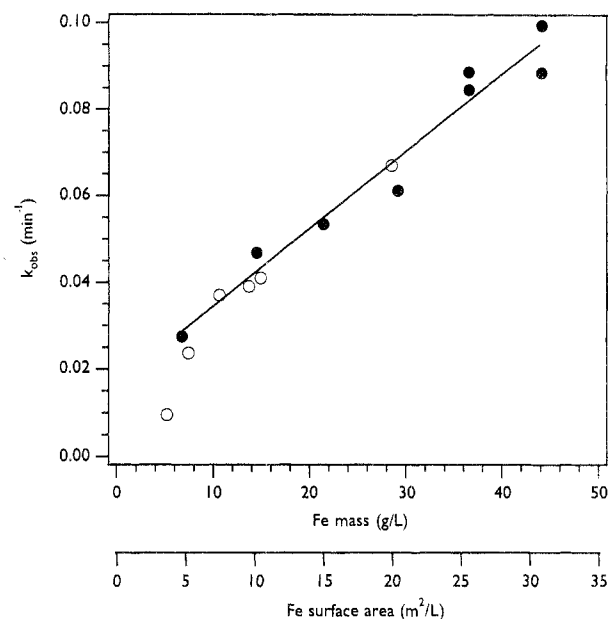
Figure 4. Effect of pH on the pseudo-first-order rate constant for carbon tetrachloride dehalogenation by iron metal. Good's buffers were used. Each bottle contained 1 g of Fisher iron powder and was mixed at 15 rpm and incubated at 15 °C. Regression line corresponds to eq 4. (O) MOPS; (□) HEPES; (△) MES; (▽) CHES; (◇) Tris.

variability on observed dehalogenation rates. A plot of log k_{obs} vs log $\{H^+\}$ also gives a linear relationship ($r^2 = 0.91$, $n = 15$, figure not shown), but in this case, the slope is the empirical order of reaction with respect to the activity of H^+. Fitting the data gives a reaction order of 0.15 ± 0.02. This low value indicates that H^+ is not involved in a single rate-determining step in the dehalogenation mechanism. It is, however, consistent with the indirect effects proposed above or with a mixture of concurrent effects.

Role of Iron Surface Characteristics. The direct role of Fe^0 as a reactant in eq 3 implies the involvement of reactive sites on the metal and, therefore, that the condition and quantity of metal surface in a reaction system should strongly influence the rate of dehalogena-

tion. Early experiments showed that preceding each experiment with rinsing of the metal in dilute aqueous HCl produced faster dechlorination and that this pretreatment was necessary to obtain any appreciable reaction at all for some iron samples. Treating the iron in this way presumably provides a well-defined and reproducible surface (16, 35), so it was applied to most experiments as a standard procedure.

The most likely explanation for the effect of acid washing is that it dissolves the surface layer on the iron grains, leaving clean reduced metal that is relatively free of unreactive oxide or organic coatings. Increased iron surface area due to corrosion may also contribute to the greater reactivity of halocarbons with acid-washed iron. However, scanning electron microscopy of the iron grains, before and after treatment with acid, showed little increase in the density of corrosion pits. Similarly, the enhanced dechlorination of acid-washed iron cannot be attributed to the effect of pH on the dehalogenation rate, because pH measurements gave no evidence for residual acidity due to the acid wash procedure.

Besides pretreatment of iron with acid, the most significant experimental variable influencing k_{obs} for dehalogenation was the amount of iron metal available to react with the organic substrate. Figure 5 illustrates this relationship in terms of two parameters: g of iron/L of reaction volume, which is operationally the most convenient, and m^2 of surface area/L, which should incorporate most of the effects of grain size and shape. The relationship appears to be linear, and regression of k_{obs} (min^{-1}) versus surface area concentration (m^2/L) gives

$$k_{obs} = 0.0025\ (\pm0.0002)\ [\text{Fe surface area}] +$$
$$0.017\ (\pm0.005)\quad (14)$$

with $r^2 = 0.96$ for $n = 8$. The concentration of iron surface area was calculated from an average specific surface area for the iron used in this experiment (0.7 m^2/g) and the

Table 4. Effects of Iron Concentration on Rate of Reductive Dehalogenation for Carbon Tetrachloride[a]

Fe before (g)	Fe after (g)[b]	vol (L)	surface area $(m^2/L)^c$	k_{obs} $(min^{-1})^d$
0.50	0.404	0.06	4.71	0.027
1.00	0.870	0.06	10.15	0.047
1.00	0.820	0.06	9.57	0.039[e]
1.00	0.814	0.11	5.18	0.029[e]
1.00	0.831	0.16	3.64	0.010[e]
1.50	1.286	0.06	15.00	0.053
2.00	1.748	0.06	20.39	0.061
2.00	1.710	0.06	19.95	0.067[e]
2.00	1.641	0.11	10.44	0.041[e]
2.00	1.695	0.16	7.42	0.037[e]
2.50	2.196	0.06	25.62	0.085
2.50	2.196	0.06	25.62	0.085
3.00	2.647	0.06	30.88	0.088
3.00	2.647	0.06	30.88	0.099

[a] Conditions: unbuffered pH $\approx$ 7, 15 °C, 15 rpm, 100-mesh Fisher electrolytic iron. [b] Weight at end of dechlorination experiment. [c] Calculated for a specific surface area = 0.7 m^2/g. [d] Standard deviations of the slope of first-order regression lines are <0.007 min^{-1}. [e] Data not included in the regression line (eq 14).

Figure 6. Effect of mixing rate on pseudo-first-order rate constant for carbon tetrachloride dehalogenation by iron metal. All contained 1 g of Fisher iron powder, were unbuffered, and were incubated at 15 °C.

mass of iron remaining after dechlorination. The robustness of eq 14 is evidenced by how well it correlates the results of a subsequent experiment in which both mass of iron and total reaction volume were varied (Table 4, Figure 5). However, the broader utility of eq 14 will be limited by the uncertain relationship between surface area determined by gas adsorption on dry samples and the concentration of accessible and reactive sites on a hydrated metal surface (36, 37). In principle, dye adsorption from aqueous solution is an alternative method for determining surface area that should offer substantial advantages for use in our systems. Unfortunately, preliminary results with this method appeared to be unreliable, and no other promising alternative to the BET method has been identified.

Kinetics of Surface Reaction. Since dehalogenation apparently occurs at the Fe/H_2O interface, transport as well as reaction steps must be involved. A general model for surface reactions consists of five steps (22, 36, 38): (i) mass transport of the reactant to the Fe^0 surface from the bulk solution; (ii) adsorption of the reactant to the surface; (iii) chemical reaction at the surface; (iv) desorption of the product(s); and (v) mass transport of the product(s) to the bulk solution. Any one or a combination of these steps may be rate limiting and, therefore, determine the values of k_{obs} obtained in this study. To properly interpret trends in the reaction rate, it is especially important to distinguish between transport- and reaction-limited kinetics.

A common criterion for detecting mass transport-limited kinetics is variation in reaction rate with intensity of mixing. Rates that are controlled by a chemical reaction step should not be affected, whereas aggressive mixing usually accelerates diffusion-controlled rates by reducing the thickness of the diffusion layer at particle surfaces (36). Batch experiments in this study were mixed by 360° rotation around a fixed-length axis, so one practical measure of mixing intensity is rpm. Figure 6 shows that k_{obs} for carbon tetrachloride reduction increased with rotation rate up to about 50 rpm. This trend suggests that mass transport is an important contributor to the kinetics of dechlorination under the conditions employed in this study. Limitations in the method of mixing did
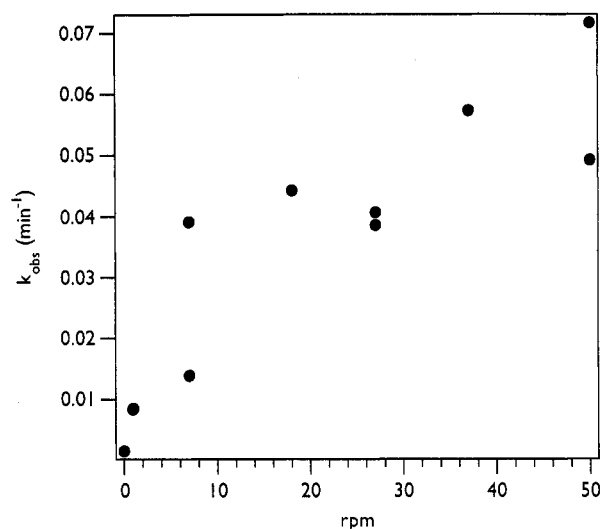
not allow a condition to be reached where mass transport was unimportant and k_{obs} was constant. Due to the uncertain form of the relationship between k_{obs} and rpm, regression has not been performed on the data. However, the trend in Figure 6 shows the importance of mixing as an experimental variable in batch studies of dehalogenation by iron.

Additional support for the importance of mass transport to the kinetics of dehalogenation in our systems comes from the effect of temperature on k_{obs}. Reaction rates that are limited by diffusion typically have low activation energies and, therefore, a weak dependence on temperature relative to rates that are limited by a chemical reaction step (36). Our data (not shown) indicate that k_{obs} is unaffected by temperature over the range from 4 to 35 °C, and fitting the data to the Arrhenius equation gives a slope that is not significantly different from zero. The practical implication of this result is that temperature control was not considered to be an important experimental variable, even though we performed most experiments at a typical groundwater temperature of 15 °C.

Mechanism of Dehalogenation. A thorough mechanistic study does not appear to have been reported on the dehalogenation of alkyl halides in dilute aqueous solution by the presence of Fe^0 or other reducing metals. However, a mechanistic context for our observations can be proposed based on the results of previous work done on a variety of related systems.

Numerous studies have shown that dissociative adsorption of H_2O takes place at clean iron metal surfaces, resulting in surface-bound hydroxyl, atomic oxygen, and atomic hydrogen (39-41). The latter species—sometimes called "nascent" hydrogen—can combine with itself, accounting for the formation of H_2, or react with other compounds in the system, resulting in their hydrogenation. Adsorbed atomic hydrogen is the species that is directly responsible for many important catalytic hydrogenation reactions (13), and it has been invoked as an intermediate in the mechanism of dissolving metal reductions (14, 42). However, dissolving metal reductions may also occur by direct electron transfer between the metal and the absorbed organic substrate. A debate over the relative importance of these two mechanisms has gone on for many

years, but the electron transfer model is generally preferred to explain reductions at the surface of metals with highly cathodic overpotentials (e.g., Fe or Zn as opposed to Pt or Pd) (14, 40, 42).

The direct reduction mechanism requires adsorption of the organic substrate on the metal surface and electron transfer. Most studies of electron transfer to alkyl halides suggest that this is a concerted, dissociative process that results in the formation of a carbon-centered radical, R$^\bullet$ (43–46):

$$RX + e^- \rightarrow R^\bullet + X^- \qquad (15)$$
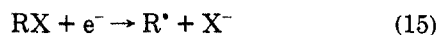
Presumably, the electron is transferred into the lowest unoccupied (σ^* antibonding) orbital of the substrate molecule (44, 47). Although the first electron transfer is rate limiting in many organic reduction reactions, this does not appear to have been the case under the conditions of this study. The initial step in corrosion of aluminum by neat chlorinated solvents is also represented by eq 15, but it has been described in different terms: as charge transfer from the metal to the halogen of the adsorbed substrate, with associated homolytic cleavage of the halogen–carbon bond (16–18). Adsorption of halocarbons from the gas phase onto iron metal surfaces is also known to occur by a dissociative mechanism, resulting in dechlorinated radicals as intermediate products (48, 49).

Once formed, the radical may react to give final products in a variety of ways. In the absence of a good proton donor, dimerization of the radical can be important, especially where the halocarbon is abundant because it is also the primary solvent (16, 50). Dimerization is not favored in dilute aqueous systems, which is consistent with the lack of hexachloroethane formation from carbon tetrachloride reduction in this study. Instead, the radical undergoes a second electron transfer and protonation, which results in the reductive dehalogenation products that we observed to be predominant:

$$R^\bullet + H^+ + e^- \rightarrow RH \qquad (16)$$

Although the rate of this step may strongly influence the observed distribution of reduction products, the reaction represented by eq 16 has received less investigation than the radical formation step (eq 15). As a result, fewer generalizations can be made about the expected effects of conditions on its rate and mechanism. For example, proton availability will certainly affect eq 16, but there is considerable uncertainty over the relationship between proton availability at the metal surface and bulk pH (47). Such distinctions may prove to be important in describing the effectiveness of iron at dehalogenating contaminants under environmental conditions.

By analogy to the mechanism of aqueous corrosion of iron (41), the half-reaction that accompanies the first electron transfer to a halocarbon (eq 15) is presumably oxidation of surface Fe^0 to Fe^{1+}. Subsequent electron transfers provide for formation and dissolution of Fe^{2+}. However, corrosion is often formulated as an electrolytic phenomenon, where the reduction half-reaction occurs at a cathodic site and oxidation occurs at an anodic site, and the two are balanced by conduction through the metal and the electrolyte (19). In highly conductive media, macroscopic separation of these sites is well known, but an electrolytic corrosion mechanism in nonionic solvent systems can only occur if site separation is very small, on

the order of angstroms, as was proposed in an early study on aluminum corrosion by boiling carbon tetrachloride (51). Others have argued that aluminum corrosion in 1,1,1-trichloroethane is not electrolytic (17) but that the oxidation and reduction half-reactions occur at the same site, i.e., without separation of anode and cathode. It is generally assumed that dissolving metal reductions, even in aqueous systems, occur without separation of anodic and cathodic sites (14). This distinction could have practical significance in the context of this study, if site separation leads to extensive pitting of the metal. However, inspection of iron surfaces by scanning electron microscopy after one of our dechlorination experiments showed very little pitting and, therefore, suggests predominantly uniform corrosion.

Conclusion

Carbon tetrachloride and chloroform undergo rapid reductive dehalogenation in the presence of fine-grained iron metal. With each successive dehalogenation, the reaction proceeds more slowly, and methylene chloride was not significantly degraded over the time scales of our experiments. Relative product distributions do vary with conditions however, so it is possible that circumstances may exist where significant degradation of methylene chloride will occur. Degradation of trichloroethylene was also observed, but the pathway for this reaction was not investigated.

In our closed model systems, the overall chemistry of the system is dominated by anaerobic corrosion; i.e., oxidative dissolution of Fe^0 to Fe^{2+}. The chloromethanes apparently substitute for water in this reaction, providing an alternative oxidant for the iron metal, and a mechanism has been proposed involving direct electron transfer to the adsorbed halocarbon. Dehalogenation of carbon tetrachloride was faster at more acidic pH, but this effect was modest. Additional effects are possible under other conditions. For example, aerobic systems may behave differently due to more aggressive corrosion and the precipitation of ferric hydroxides; sulfide, where it occurs in groundwater, will significantly influence the redox chemistry of iron and probably also the fate of chlorinated contaminants; and bacteria could be important due to microbial dehalogenation, biocorrosion, Fe^{2+} oxidation, or Fe^{3+} reduction.

Under the conditions of our experiments, mass transport of substrate to the iron surface appeared to be an important determinant of the dechlorination rate, so it was necessary to control mixing as an experimental parameter. The most important predictor of dechlorination rate was found to be iron surface area concentration. Even during environmental application it is likely that access to, condition of, and concentration of the iron surface will be the dominant factors controlling remediation performance.

vided by the Strategic Environmental Research and Development Program (SERDP) of DoD, DoE, and EPA. This paper has not been subject to review by the U.S. Environmental Protection Agency and, therefore, does not necessarily reflect the views of the Agency, and no official endorsement should be inferred.

Literature Cited

(1) Senzaki, T.; Yasuo, K. *Kogyo Yosui* **1988**, 2–7.
(2) Senzaki, T.; Yasuo, K. *Kogyo Yosui* **1989**, 19–25.
(3) Senzaki, T. *Kogyo Yosui* **1991**, *391*, 29–35.
(4) Sweeny, K. H. *Water Reuse Symposium*; American Water Works Association Research Foundation: Denver, 1979; Vol. 2, pp 1487–1497.
(5) Sweeny, K. H. *AIChE Symp. Ser.* **1981**, *77*, 72–78.
(6) Erickson, M. D.; Estes, E. D. *Evaluation of chlorinated hydrocarbon catalytic reduction technology*; U.S. Environmental Protection Agency: Research Triangle Park, NC, 1978; Task Final Report; EPA-600/2-78-059,
(7) Reynolds, G. W.; Hoff, J. T.; Gillham, R. W. *Environ. Sci. Technol.* **1990**, *24*, 135–142.
(8) Orth, W. S. M.S. Thesis Thesis, University of Waterloo, Ontario, 1993.
(9) Gillham, R. W.; O'Hannesin, S. F. *Ground Water* **1994**, *32*, 958–967.
(10) O'Hannesin, S. F. M.S. Thesis Thesis, University of Waterloo, Ontario, 1993.
(11) Bratsch, S. G. *J. Phys. Chem. Ref. Data* **1989**, *18*, 1–21.
(12) Vogel, T. M.; Criddle, C. S.; McCarty, P. L. *Environ. Sci. Technol.* **1987**, *21*, 722–736.
(13) Hudlický, M. *Reductions in Organic Chemistry*; Ellis Horwood: Chichester, 1984; p 309.
(14) House, H. O. *Modern Synthetic Reactions*, 2nd ed.; W. A. Benjamin: Menlo Park, CA, 1972; pp 145–227.
(15) Rhodes, F. H.; Carty, J. T. *Ind. Eng. Chem.* **1925**, *17*, 909–911.
(16) Archer, W. L.; Simpson, E. L. *Ind. Eng. Chem. Prod. Res. Dev.* **1977**, *16*, 158–162.
(17) Archer, W. L. *Ind. Eng. Chem. Prod. Res. Dev.* **1982**, *21*, 670–672.
(18) Archer, W. L.; Harter, M. K. *Corrosion* **1978**, *34*, 159–162.
(19) Jones, D. A. *Principles and Prevention of Corrosion*; Macmillan: New York, 1992; p 7.
(20) Doong, R.-A.; Wu, S.-C. *Chemosphere* **1992**, *24*, 1063–1075.
(21) Klečka, G. M.; Gonsior, S. J. *Chemosphere* **1984**, *13*, 391–402.
(22) Stumm, W. *Chemistry of the Solid–Water Interface: Processes at the Mineral–Water and Particle–Water Interface of Natural Systems*; Wiley: New York, 1992; 428 pp.
(23) Pankow, J. F.; Rosen, M. E. *Environ. Sci. Technol.* **1988**, *22*, 398–405.
(24) Grob, K.; Küffer, F. *J. High Resolut. Chromatogr.* **1990**, *13*, 561–564.
(25) Gibbs, M. M. *Water Res.* **1979**, *13*, 295–297.
(26) Light, T. S. *Anal. Chem.* **1972**, *44*, 1038–1039.
(27) Wackett, L. P.; Logan, M. S. P.; Blocki, F. A.; Cai, B.-L. *Biodegradation* **1992**, *3*, 19–36.
(28) Larson, R. A.; Weber, E. J. *Reaction Mechanisms in Environmental Organic Chemistry*; Lewis: Chelsea, MI, 1993.
(29) Jeffers, P. M.; Ward, L. M.; Woytowitch, L. M.; Wolfe, N. L. *Environ. Sci. Technol.* **1989**, *23*, 965–969.
(30) Kriegman-King, M. R.; Reinhard, M. *Environ. Sci. Technol.* **1992**, *26*, 2198–2206.
(31) Criddle, C. S.; McCarty, P. L. *Environ. Sci. Technol.* **1991**, *25*, 973–978.
(32) Capellos, C.; Bielski, B. H. J. *Kinetic Systems: Mathematical Descriptions of Chemical Kinetics in Solution*; Wiley: New York, 1972; p 138.
(33) Cannon, R. D. *Electron Transfer Reactions*; Butterworth: London, 1980.
(34) Good, N. E.; Winget, G. D.; Winter, W.; Connolly, T. N.; Izawa, S.; Singh, R. M. M. *Biochemistry* **1966**, *5*, 467–477.
(35) *Metals Handbook, Vol. 5: Surface Cleaning, Finishing, and Coating*, 5th ed.; Wood, W. G., Ed.; American Society for Metals: Metals Park, OH, 1982.
(36) Spiro, M. In *Chemical Kinetics*; Compton, R. G., Ed.; Elsevier: Amsterdam, 1989; Vol. 28, Reactions at the Liquid-Solid Interface; pp 69–166.
(37) van den Hul, H. J.; Lyklema, J. *J. Am. Chem. Soc.* **1968**, *90*, 3010–3015.
(38) Stone, A. T.; Morgan, J. J. In *Aquatic Chemical Kinetics*; Stumm, W., Ed.; Wiley: New York, 1990; pp 1–41.
(39) Hung, W.-H.; Schwartz, J.; Bernasek, S. L. *Surf. Sci.* **1991**, *248*, 332–342.
(40) Thiel, P. A.; Madey, T. E. *Surf. Sci. Rep.* **1987**, *7*, 211–385.
(41) Bockris, J. O.; Khan, S. U. M. *Surface Electrochemistry. A Molecular Level Approach*; Plenum: New York, 1993; p 1014.
(42) Brewster, J. H. *J. Am. Chem. Soc.* **1954**, *76*, 6361–6363.
(43) Eberson, L. *Acta Chem. Scand.* **1982**, *B36*, 533–543.
(44) Walborsky, H. M.; Hamdouchi, C. *J. Am. Chem. Soc.* **1993**, *115*, 6406–6408.
(45) Hush, N. S. *Z. Elektrochem.* **1957**, *61*, 734–738.
(46) Savéant, J. M. *J. Am. Chem. Soc.* **1992**, *114*, 10595–10602.
(47) Casanova, J.; Eberson, L. In *The Chemistry of the Carbon-Halogen Bond, Part 2*; Patai, S., Ed.; Wiley: London, 1973; pp 979–1047.
(48) Smentkowski, V. S.; Cheng, C. C.; Yates, J. T. J. *Langmuir* **1990**, *6*, 147–158.
(49) Grunze, M.; Dowben, P. A. *Appl. Surf. Sci.* **1982**, *10*, 209–239.
(50) Stern, M.; Uhlig, H. H. *J. Electrochem. Soc.* **1953**, *100*, 543–551.
(51) Brown, R. H.; Cook, E. H.; Brown, M. H.; Minford, J. D. *J. Electrochem. Soc.* **1959**, *106*, 192–199.